

Study on the Light Scattering from Random Rough Surfaces by Kirrhoff Approximation

¹ Keding Yan, ² Shu Jiang, ¹ Zhenhua Li

¹ Department of Information Physics & Engineering, Nanjing University of Science & Technology, Nanjing 210094, China

² 704 Institute, China Shipbuilding Industry Corporation, Shanghai, 200031, China
E-mail: yankeding168@gmail.com

Received: 7 June 2014 / Accepted: 30 June 2014 / Published: 31 July 2014

Abstract: In order to study the space distribution characteristics of light scattering from random rough surfaces, the linear filtering method is used to generate a series of Gaussian randomly rough surfaces, and the Kirchhoff Approximation is used to calculate the scattered light intensity distribution from random metal and dielectric rough surfaces. The three characteristics of the scattered light intensity distribution peak, the intensity distribution width and the position of peak are reviewed. Numerical calculation results show that significant differences between scattering characteristics of metal surfaces and the dielectric surfaces exist. The light scattering characteristics are jointly influenced by the slope distribution and reflectance of surface element. The scattered light intensity distribution is affected by common influence of surface local slope distribution and surface local reflectivity. The results can provide a basis theory for the research to lidar target surface scattering characteristics. *Copyright © 2014 IFSA Publishing, S. L.*

Keywords: Light scattering, Random rough surface, Kirchhoff approximation.

1. Introduction

Light scattering from rough surfaces has been studied for long time, and it keeps attracting a great deal of attention from the scientific and technological community. Many important applications in our society rely on such knowledge such as remote sensing, optical detection, lidar detection [1-3]. The research on light scattering from rough surface can provide useful information such as target spectrum, reflection coefficient of intensity, depolarization of scattered light for lidar [4]. Numerical studies of light scattering from target surfaces would contribute to a better understanding of light scattering from the surfaces and could get more information of target from lidar scattering.

Many different algorithms of solving scattered field are proposed including small perturbation method (SPM) [5, 6], method of moments (MoM) [7-9], and Kirchhoff Approximation(KA) [10-12], *etc.* P. Letnes *et al.* calculated the Mueller matrix of the two-dimensional random rough surfaces by SPM. I. Simonsen *et al.* introduced MoM simulations of wave scattering from perfect conducting surfaces. But there are few articles to research the mechanism of scattering characteristic. In this paper, the linear filtering method is used to generate Gaussian randomly rough surface, scattered light intensity space distribution in the condition of the s- and p-polarized incident light are calculated by KA. With analyzing the space distribution of scattered light intensity from a series of surfaces at different

materials, we find the scattering characteristic have different intensity changing tendency in p- and s-polarized occasions. Theoretical analysis of scattering characteristic mechanism of the light scattering from randomly rough dielectrics and metal surfaces is also proposed in this paper. This method will provide more reference for target and identification in laser radar and remote sensing, etc.

2. Solve Scattered Field by KA

Compared to SPM and MoM, KA owns much higher calculation efficiency in time consuming and polarization setting freedom [13, 14], so we choose KA to Solve scattered field. There are mainly three steps in solving scattered field by KA. Firstly, the rough surfaces need to be generated with filtering method. Then, local fields of the rough surface are calculated. Next step is using the local fields of the rough surface to calculate light scattering via Stratton-Chu equation.

2.1. Generate 1-D Random Rough Surfaces via Filtering Method

The randomly rough surfaces could be generated by the sum of sinusoidal waves with different frequencies. Therefore, linear filtering method is applied to generate these 1-D randomly rough surfaces. In this work the Surface profile function $z(x)$ is assumed to be a single-valued function of x that constitutes a stationary, zero-mean, Gaussian random process defined by $\langle z(x)z(x') \rangle = \delta^2 S(|x-x'|)$, where the angle brackets denote an average over the ensemble of realizations of the surface profile function, and $\delta = \langle z^2(x) \rangle^{1/2}$ is the rms height of the surface. We will assume a Gaussian form for $S(|x-x'|) = \exp[-(x-x')^2/T^2]$, where T is the correlation length of the surface roughness. Each realization of the surface, profile function with these properties is generated numerically by filtering method used in [15, 16].

The randomly rough surface can be considered as superposition of many different frequency harmonics, so the randomly rough surface can be obtained by linear filtering method [9]. The one-dimensional randomly rough surface with the length L can be expressed as:

$$f(x_n) = \frac{1}{L} \sum_{j=-N/2+1}^{N/2} F(k_j) \exp(ikx_n), \quad (1)$$

where $x_n = n\Delta x$ ($n = -N/2+1, \dots, N/2$) is the n -th sampling point, $F(k_j)$ is the FFT of $f(x_n)$, and can be expressed as:

$$F(k_j) = \frac{2\pi}{\sqrt{2\Delta k}} \sqrt{S(k_j)} \begin{cases} [N(0,1) + iN(0,1)], j = -N/2+1, \dots, -1 \\ N(0,1), j = 0, N/2 \end{cases} \quad (2)$$

When $j > 0$, $F(k_j) = F(k_{-j})^*$. k_j is the wave number

$$k_j = 2\pi j/L, \quad (3)$$

Δk is the difference of wave number. The power spectral density of Gauss is

$$S(k_j) = \delta^2 l / (2\sqrt{\pi}) \exp(-k_j^2/4), \quad (4)$$

In equation (4), $N(0,1)$ is Gauss distributed randomly numbers.

Fig. 1 shows one example of randomly rough surfaces, the wavelength of the incident wave is $\lambda = 1.064\mu m$, the RMS $\delta = 0.2\lambda$, the correlation length $T = 2\lambda$, the sampling points are $N = 2048$ and the length of the 1-D randomly rough surface is $L = 100\lambda$.

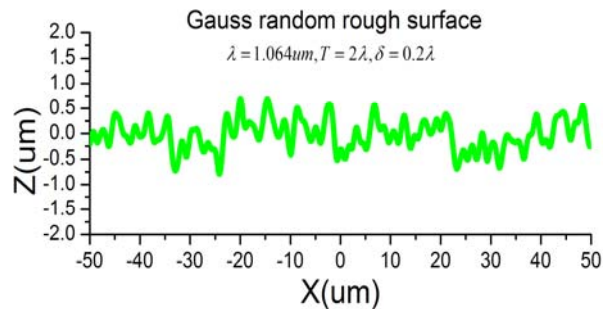


Fig. 1. 1-D Gaussian distributed randomly rough surface.

2.2. Solve the Local Fields of the Rough Surface

In order to solve the local fields $E(r')$ at every point on the rough surface, Kirchhoff approximation is applied as the boundary condition, and the local field as the sum of the incident light and the reflective light from the tangent of that point. The reflective light could be calculated via Fresnel reflective coefficient. The geometry relationship in light scattering from randomly rough surface is shown in Fig. 2.

Suppose the plane wave is illuminated at a randomly rough surface, k_i is the light vector of incident wave $k_i = k \sin\theta_i \mathbf{x} - k \cos\theta_i \mathbf{z}$, $k = 2\pi/\lambda$ and k_s is the light vector of incident wave $k_s = k \sin\theta_s \mathbf{x} - k \cos\theta_s \mathbf{z}$, θ_i and θ_s are incident and scattering angles, respectively. The fields of the incident wave are:

$$E_i(\mathbf{r}') = e_i \exp[i\mathbf{k}_i \cdot \mathbf{r}'], \quad (5)$$

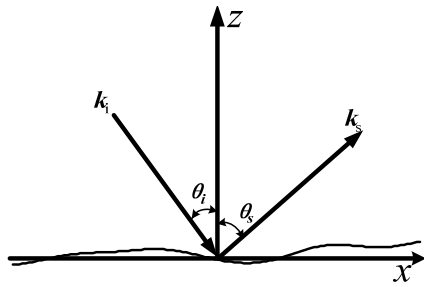


Fig. 2. The geometry relationship in light scattering from randomly rough surface.

In equation (5), e_i is the unit vector of the incident wave, k is the wave number of the light wave. \mathbf{r}' is the point of the rough surface which could be expressed as $\mathbf{r}' = x'\mathbf{x} + z'\mathbf{z}$.

The geometry relationship of local surface ds' is shown in Fig 3. \mathbf{n} is the normal unit vector of the local fields,

$$\mathbf{n} = \frac{1}{\sqrt{1 + (dz/dx)^2}} \left(-\frac{dz}{dx} \mathbf{x} + \mathbf{z} \right), \quad (6)$$

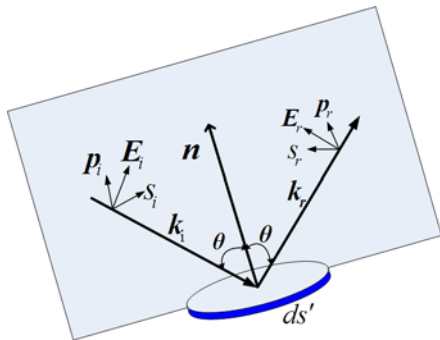


Fig. 3. The geometry relationship of local surface ds' .

The local fields of the incident wave are:

$$E_i(\mathbf{r}') = (A_{pi} \mathbf{p}_i + A_{si} \mathbf{s}_i) \exp[i\mathbf{k}_i \cdot \mathbf{r}'], \quad (7)$$

where \mathbf{k}_i and \mathbf{n} constitute a local incident plane, \mathbf{s}_i is the unit vector vertical to the local incident plane,

$$\mathbf{s}_i = \frac{\mathbf{n} \times \mathbf{k}_i}{|\mathbf{n} \times \mathbf{k}_i|}, \quad (8)$$

where \mathbf{p}_i is the unit parallel to the local incident plane,

$$\mathbf{p}_i = \frac{\mathbf{k}_i \times \mathbf{s}_i}{|\mathbf{k}_i \times \mathbf{s}_i|}, \quad (9)$$

where \mathbf{k}_r and \mathbf{n} constitute a local reflective plane, \mathbf{k}_r is the light vector of local reflective wave,

$$\mathbf{k}_r = \mathbf{k}_i - 2(\mathbf{k}_i \cdot \mathbf{n})\mathbf{n}, \quad (10)$$

where θ is the local incident angle

$$\theta = \arccos \left(\frac{-\mathbf{k}_i \cdot \mathbf{n}}{|\mathbf{k}_i| |\mathbf{n}|} \right), \quad (11)$$

where \mathbf{s}_r is the unit vector vertical to the local scattering plane,

$$\mathbf{s}_r = \frac{\mathbf{n} \times \mathbf{k}_r}{|\mathbf{n} \times \mathbf{k}_r|}, \quad (12)$$

where \mathbf{p}_r is the unit vector parallel to the local scattering plane,

$$\mathbf{p}_r = \frac{\mathbf{k}_r \times \mathbf{s}_r}{|\mathbf{k}_r \times \mathbf{s}_r|}, \quad (13)$$

The reflective fields could be calculated by Fresnel formula

$$E_r(\mathbf{r}') = (r_p A_{pi} \mathbf{p}_r + r_s A_{si} \mathbf{s}_r) \exp[i\mathbf{k}_i \cdot \mathbf{r}'], \quad (14)$$

The reflective coefficient of p-component is

$$r_p = \frac{(n_0^2 \cos \theta - n_a)}{(n_0^2 \cos \theta + n_a)}, \quad (15)$$

and the reflective coefficient of s-component is

$$r_s = \frac{(\cos \theta - n_a)}{(\cos \theta + n_a)}, \quad (16)$$

and

$$n_a = \sqrt{n_0^2 - \sin^2 \theta}, \quad (17)$$

Then, based on the boundary condition of Stratton-Chu equation and Kirchhoff approximation, the local fields of each unit area are explained as:

$$E(\mathbf{r}') = [E_{si}(\mathbf{s}_i + r_s \mathbf{s}_r) + E_{pi}(\mathbf{p}_i + r_p \mathbf{p}_r)] \exp(i\mathbf{k}_i \cdot \mathbf{r}'), \quad (18)$$

After solving $E(\mathbf{r}')$, spatial scattered fields $E^S(\mathbf{r})$ could be obtained according to Stratton-Chu equation.

2.3. Solve the Scattered Fields by Stratton-Chu equation

Stratton-Chu equation is proposed to calculate the spatial scattered fields by using integral to solve the scattered fields from local fields of each point on the rough surfaces.

Thus, scattered fields of 1-D randomly rough surfaces could be obtained. The Stratton-Chu equation is shown in Equation (19).

$$\mathbf{E}^S(\mathbf{r}) = \frac{1}{4\pi s} \int \{ \hat{\mathbf{n}} \times [\nabla \times \mathbf{E}(\mathbf{r}')] G(\mathbf{r}, \mathbf{r}') + [\hat{\mathbf{n}} \times \mathbf{E}(\mathbf{r}')] \times \nabla G(\mathbf{r}, \mathbf{r}') + [\hat{\mathbf{n}} \cdot \mathbf{E}(\mathbf{r}')] \nabla G(\mathbf{r}, \mathbf{r}') \} ds' \quad (19)$$

In Equation (19), $\mathbf{E}(\mathbf{r}')$ is the local field, \mathbf{r}' is the vector of 1-D randomly rough surfaces, \mathbf{n} is the normal vector of the local point. ds' is the unit area of randomly rough surfaces, $\mathbf{E}^S(\mathbf{r})$ is the scattered field and r is the vector of any point in the space.

$$\nabla \times \mathbf{E}(\mathbf{r}') = i [A_{pi}(\mathbf{k}_i \times \mathbf{p}_i + r_p \mathbf{k}_r \times \mathbf{p}_r) + A_{si}(\mathbf{k}_i \times \mathbf{s}_i + r_s \mathbf{k}_r \times \mathbf{s}_r)] \exp(i\mathbf{k}_i \cdot \mathbf{r}') \quad (20)$$

$$\mathbf{n} \times [\nabla \times \mathbf{E}(\mathbf{r}')] G(\mathbf{r}, \mathbf{r}') = \frac{i \exp(ikr) \exp[i(\mathbf{k}_i - \mathbf{k}_s) \cdot \mathbf{r}']}{r} \{ A_{pi} [\mathbf{n} \times (\mathbf{k}_i \times \mathbf{p}_i) + r_p \mathbf{n} \times (\mathbf{k}_r \times \mathbf{p}_r)] + A_{si} [\mathbf{n} \times (\mathbf{k}_i \times \mathbf{s}_i) + r_s \mathbf{n} \times (\mathbf{k}_r \times \mathbf{s}_r)] \} \quad (23)$$

According to $(\mathbf{a} \times \mathbf{b}) \times \mathbf{c} = (\mathbf{c} \cdot \mathbf{a})\mathbf{b} - (\mathbf{c} \cdot \mathbf{b})\mathbf{a}$, we have:

$$\mathbf{n} \times [\nabla \times \mathbf{E}(\mathbf{r}')] G(\mathbf{r}, \mathbf{r}') = \frac{i \exp(ikr) \exp[i(\mathbf{k}_i - \mathbf{k}_s) \cdot \mathbf{r}']}{r} \{ A_{pi} [(\mathbf{n} \cdot \mathbf{p}_i)\mathbf{k}_i - (\mathbf{n} \cdot \mathbf{k}_i)\mathbf{p}_i + r_p(\mathbf{n} \cdot \mathbf{p}_r)\mathbf{k}_r - r_p(\mathbf{n} \cdot \mathbf{k}_r)\mathbf{p}_r] + A_{si} [(\mathbf{n} \cdot \mathbf{s}_i)\mathbf{k}_i - (\mathbf{n} \cdot \mathbf{k}_i)\mathbf{s}_i + r_s(\mathbf{n} \cdot \mathbf{s}_r)\mathbf{k}_r - r_s(\mathbf{n} \cdot \mathbf{k}_r)\mathbf{s}_r] \} \quad (24)$$

In a similar way we have:

$$[\mathbf{n} \times \mathbf{E}(\mathbf{r}')] \times \nabla G(\mathbf{r}, \mathbf{r}') = \frac{-i \exp(ikr) \exp[i(\mathbf{k}_i - \mathbf{k}_s) \cdot \mathbf{r}']}{r} \{ A_{pi} [(\mathbf{n} \cdot \mathbf{k}_s)\mathbf{p}_i + r_p(\mathbf{n} \cdot \mathbf{k}_s)\mathbf{p}_r] + A_{si} [(\mathbf{n} \cdot \mathbf{k}_s)\mathbf{s}_i + r_s(\mathbf{n} \cdot \mathbf{k}_s)\mathbf{s}_r] - A_{pi} [\mathbf{k}_s \cdot (\mathbf{p}_i + r_p \mathbf{p}_r)] \mathbf{n} - A_{si} [\mathbf{k}_s \cdot (\mathbf{s}_i + r_s \mathbf{s}_r)] \mathbf{n} \} \quad (25)$$

$$[\mathbf{n} \cdot \mathbf{E}(\mathbf{r}')] \nabla G(\mathbf{r}, \mathbf{r}') = \frac{-i \exp(ikr) \exp[i(\mathbf{k}_i - \mathbf{k}_s) \cdot \mathbf{r}']}{r} \{ A_{pi} [\mathbf{n} \cdot (\mathbf{p}_i + r_p \mathbf{p}_r)] \mathbf{k}_s + A_{si} [\mathbf{n} \cdot (\mathbf{s}_i + r_s \mathbf{s}_r)] \mathbf{k}_s \} \quad (26)$$

At last Stratton-Chu equation is changed into:

$$\mathbf{E}^S(\mathbf{r}) = \frac{i \exp(ikr)}{4\pi r} \iint (A_1 + A_2 + A_3 + A_4) \exp[i(\mathbf{k}_i - \mathbf{k}_s) \cdot \mathbf{r}'] \frac{dx dy}{\sqrt{1 + (\partial z / \partial x)^2 + (\partial z / \partial y)^2}}$$

$$\begin{aligned} A_1 &= [(A_{pi} \mathbf{p}_i + A_{si} \mathbf{s}_i) \cdot (\mathbf{k}_i - \mathbf{k}_s) + (A_{pi} r_p \mathbf{p}_r + A_{si} r_s \mathbf{s}_r) \cdot (\mathbf{k}_r - \mathbf{k}_s)] \mathbf{n} \\ A_2 &= -[\mathbf{n} \cdot (A_{pi} \mathbf{p}_i + A_{si} \mathbf{s}_i)] (\mathbf{k}_i + \mathbf{k}_s) \\ A_3 &= -[\mathbf{n} \cdot (A_{pi} r_p \mathbf{p}_r + A_{si} r_s \mathbf{s}_r)] (\mathbf{k}_r + \mathbf{k}_s) \\ A_4 &= (\mathbf{n} \cdot \mathbf{k}_s) [(A_{pi} \mathbf{p}_i + A_{si} \mathbf{s}_i) + (A_{pi} r_p \mathbf{p}_r + A_{si} r_s \mathbf{s}_r)] \end{aligned} \quad (27)$$

3. Numerical Simulations

3.1. Dielectrics Surfaces

In this simulation we calculate the ensemble average of scattered fields of 10^5 random rough surfaces each roughness parameter list in Table 1 and Table 2. The wavelength of the incident light which is 1064 nm in this simulation, 1-D randomly rough surfaces are generated with a length of 100λ . The

$G(\mathbf{r}, \mathbf{r}')$ is the Green function

$$G(\mathbf{r}, \mathbf{r}') = \frac{\exp(ikr) \exp(-i\mathbf{k}_s \cdot \mathbf{r}')}{r} \quad (21)$$

$\nabla G(\mathbf{r}, \mathbf{r}')$ is:

$$\nabla G(\mathbf{r}, \mathbf{r}') = \frac{-i \exp(ikr) \exp(-i\mathbf{k}_s \cdot \mathbf{r}')}{r} \mathbf{k}_s \quad (22)$$

According to equation (20) and (21), we have:

whole simulation is applying Fortran compiler with computer based calculation platform (Intel i5, 3.40 GHz, 16 GB RAM).

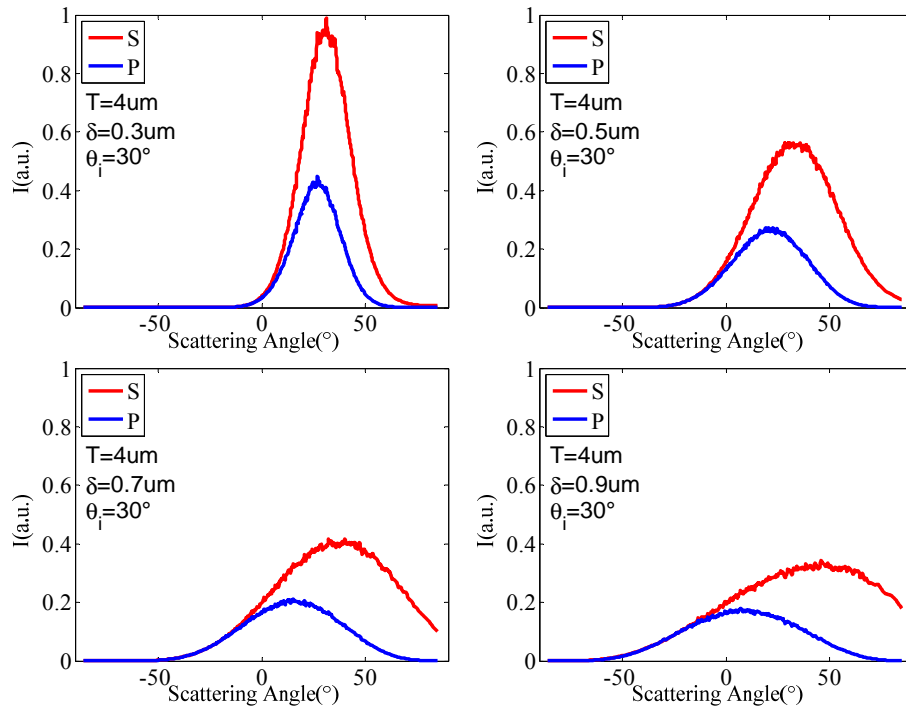
Fig. 4 show the angle distribution of scattered light from randomly rough K5 glass dielectric surfaces in p- and s- polarized light in the roughness parameters are show in Table 1, and the incident angles are set 30 degree. The dielectric model is chose as K5 glass whose refractive index is 1.52 [17].

Table 1. Roughness parameters of surfaces.

Surfaces	$\delta/\mu\text{m}$	$T/\mu\text{m}$
A	0.3 μm	4 μm
B	0.5 μm	4 μm
C	0.7 μm	4 μm
D	0.9 μm	4 μm

Table 2. Roughness parameters of surfaces.

Surfaces	$\delta/\mu\text{m}$	$T/\mu\text{m}$
E	0.3 μm	3.2 μm
F	0.5 μm	3.2 μm
G	0.7 μm	3.2 μm
H	0.9 μm	3.2 μm

**Fig. 4.** Numerical simulation of scattered light intensity from K5 glass dielectric surfaces. Incident angle is 30° , correlation length $T=4 \mu\text{m}$.

The three scattering characteristics of the scattered light intensity distribution peak, the intensity distribution width and the position of peak are reviewed.

It can be seen that both the intensity distribution width of s- and p- light are broadening obviously with the increase of roughness; Both the scattered light intensity distribution peak of s- and p- light decrease with the increase of rms height, but the peak of s-light is larger than peak of p- light at the same rms height; Both position of peak of s- and p- light are in the specular angle direction when $\delta=0.3 \mu\text{m}$, then s-light shifts from specular to large scattering angle direction with the increase of roughness, but peak position shifts from specular to backscattering direction with the increase of roughness.

Fig. 5 show the angle distribution of scattered light from randomly rough K5 glass dielectric surfaces in p- and s- polarized light in the roughness parameters are show in Table 2, and the incident angles are set 20 degree.

The three scattering characteristics shown in Fig. 5 are similar to characteristics shown in Fig. 4.

3.2. Metal Surfaces

Here, we chose iron surfaces as the targets. The refractive index at 1064 nm of iron is $3.24+4.26i$ [17]. Fig. 6 shows the angle distribution of scattered light from randomly rough iron metal surfaces in p- and s- polarized light in the roughness parameters (are show in Table 1), and the incident angles are set 30 degree.

Similar to the randomly rough metal surface, the light distribution characteristic scattering from dielectric surfaces can be described by scattered light distribution width, scattered light peak value, and the peak position.

With the increase of roughness, distribution width are broadening; Both peak value of s- and p- polarized incident light decrease with the increase of rms height, but the peak value of s- polarized incident light is larger than peak value of p- polarized incident light at the same rms height; Peak position of s- polarized incident light and peak position of p- polarized incident light are almost in the specular direction.

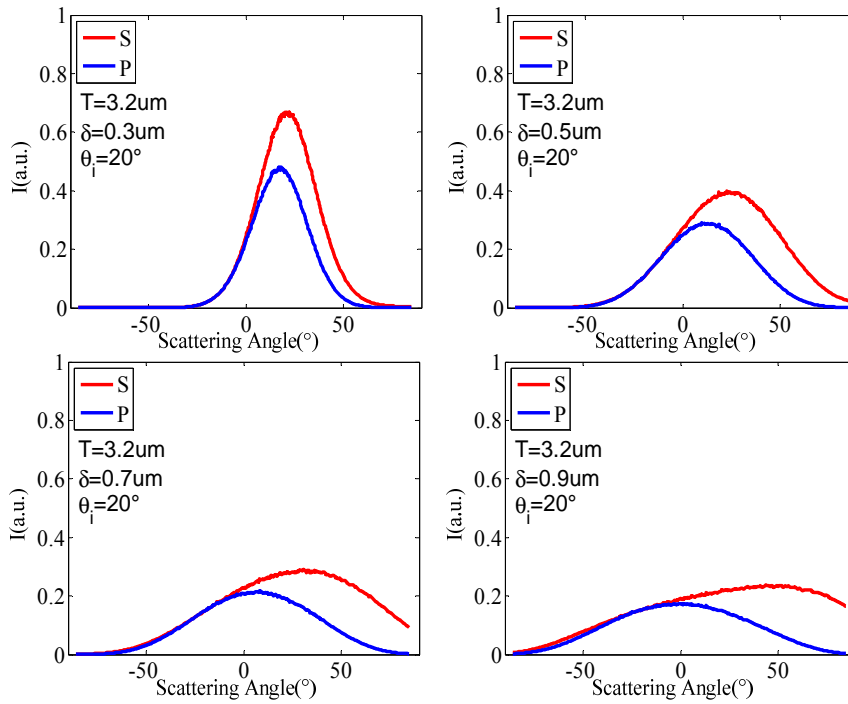


Fig. 5. Numerical simulation of scattered light intensity from K5 glass dielectric surfaces. Incident angle is 20° , correlation length $T=3.2 \mu m$.

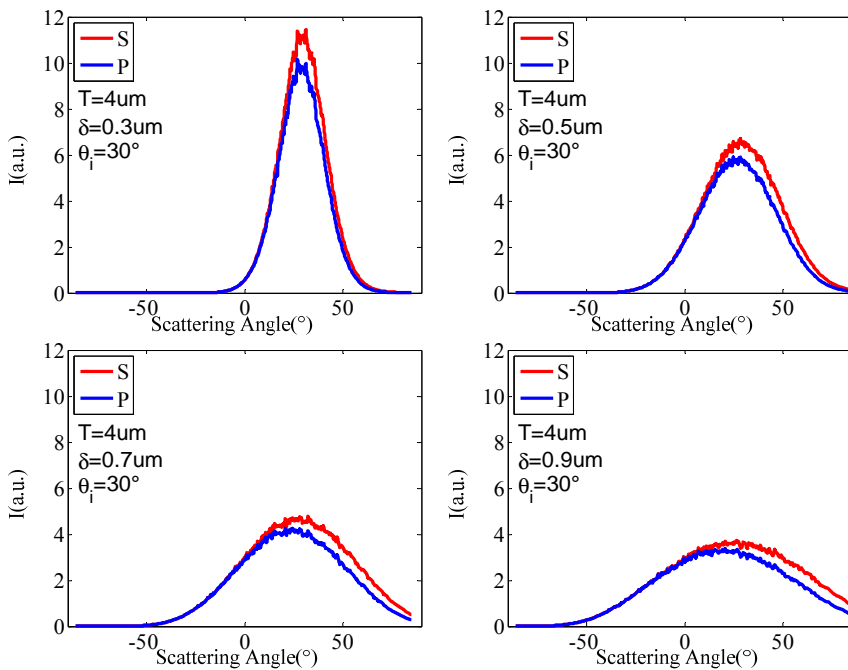


Fig. 6. Numerical simulation of scattered light intensity from iron surfaces. Incident angle is 30° , correlation length $T=4 \mu m$.

Fig. 7 show the angle distribution of scattered light from randomly rough iron metal surfaces in p- and s- polarized light in the roughness parameters are show in Table 2, and the incident angles are set 20 degree.

The numerical simulation above show that space distribution scattering characteristics between metal and dielectric surfaces exist three significant differences: first, the scattering peak value of metal is

larger than scattering peak value of dielectric on the same roughness; secondly, the difference between s- and p-light scattering results are rather small in metal randomly rough surfaces, while there is a obvious difference between s- and p-polarized scattering results in the condition of dielectric randomly rough surfaces; Thirdly, though in both conditions of metal and dielectric randomly rough surfaces, there is a shift from specular to

backscattering direction when incident is p-polarized light, however, in dielectric randomly rough surface situation, the shift is much more obvious than in metal situation.

4. Theoretical Analyses

The scattered fields are the sum of incident fields and local reflective fields in KA. When the incident and scattering angles, θ_i and θ_s are determined, scattered fields are decided by the slope and the reflective coefficient of the local unit area of randomly rough surfaces and the scattered fields are

mostly contributed by those unit areas whose θ_i and θ_s are satisfying the reflective law. The local incident angles of incident wave of the unit areas which should be $\theta=(\theta_i+\theta_s)/2$ are equal to the local scattering angles. Because the distributions of the randomly rough surfaces satisfy the Gaussian distribution, the probability density of the unit area slopes is:

$$p(s) = \frac{1}{\sqrt{\pi}\sigma_s} \exp\left(-\frac{s^2}{2\sigma_s^2}\right), \quad (28)$$

where $s=dz/dx=\tan((\theta_i-\theta_s)/2)$, and $\sigma_s = \sqrt{2}\sigma/T$.

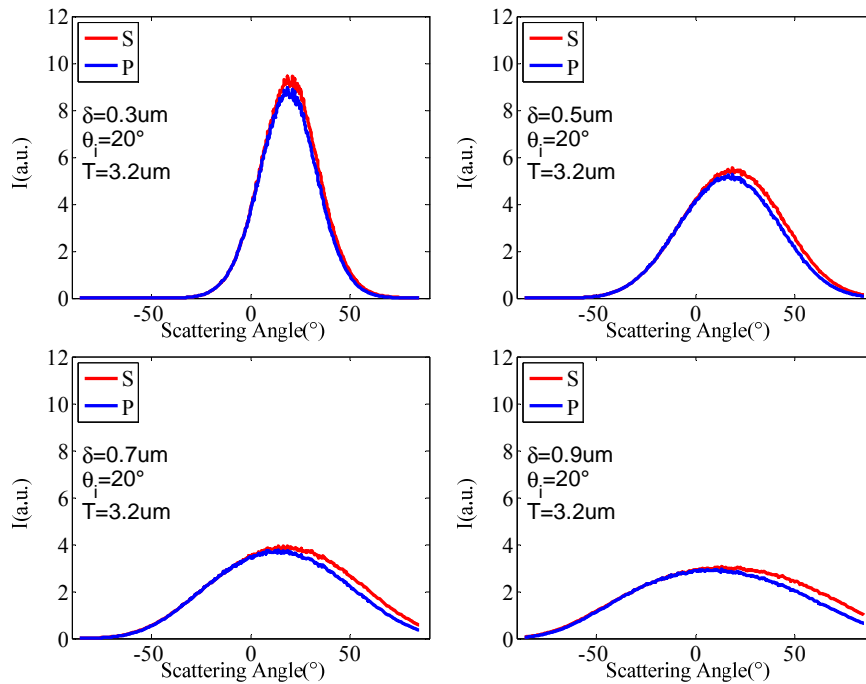


Fig. 7. Numerical simulation of scattered light intensity from iron surfaces. Incident angle is 20°, correlation length $T=3.2 \mu m$.

When the incident angle is decided, the reflective coefficients of the local unit areas are depended on the scattering angles. The reflective coefficients of p- and s-polarization are shown as:

$$r_p = \frac{n_0 \cos((\theta_i + \theta_s)/2) - \sqrt{n_0^2 - \sin^2((\theta_i + \theta_s)/2)}}{n_0 \cos((\theta_i + \theta_s)/2) + \sqrt{n_0^2 - \sin^2((\theta_i + \theta_s)/2)}}, \quad (29)$$

$$r_s = \frac{\cos((\theta_i + \theta_s)/2) - \sqrt{n_0^2 - \sin^2((\theta_i + \theta_s)/2)}}{\cos((\theta_i + \theta_s)/2) + \sqrt{n_0^2 - \sin^2((\theta_i + \theta_s)/2)}}, \quad (30)$$

Local reflectivity of p-polarization light $R_p = |r_p|^2$ and local reflectivity of s-polarization light $R_s = |r_s|^2$. The theoretical distributions of the

scattering characteristic is due to and distribution of local slope $p(s)$, the total effect I'_p and I'_s are

$$\begin{aligned} I'_p &= R_p p(s) \\ I'_s &= R_s p(s) \end{aligned}, \quad (31)$$

4.1. Dielectric Surfaces

Fig. 8 compare the numerical simulated and theoretical analysis of scattered field of 1-D randomly rough K5 glass dielectric surfaces when incident light is S light. Fig. 9 compare the numerical simulated and theoretical analysis of scattered field of 1-D randomly rough K5 glass dielectric surfaces when incident light is P light.

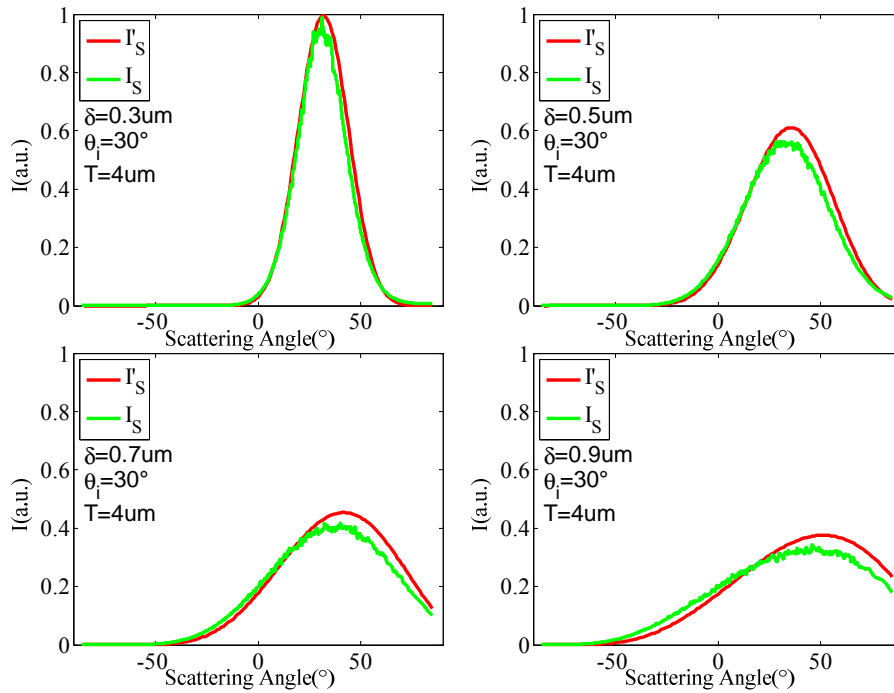


Fig. 8. The comparison between numerical simulation results and theoretical analysis of scattered light intensity from K5 glass dielectric surfaces. Incident light is S light, and the incident angle is 30° , the correlation length $T=4\text{um}$.

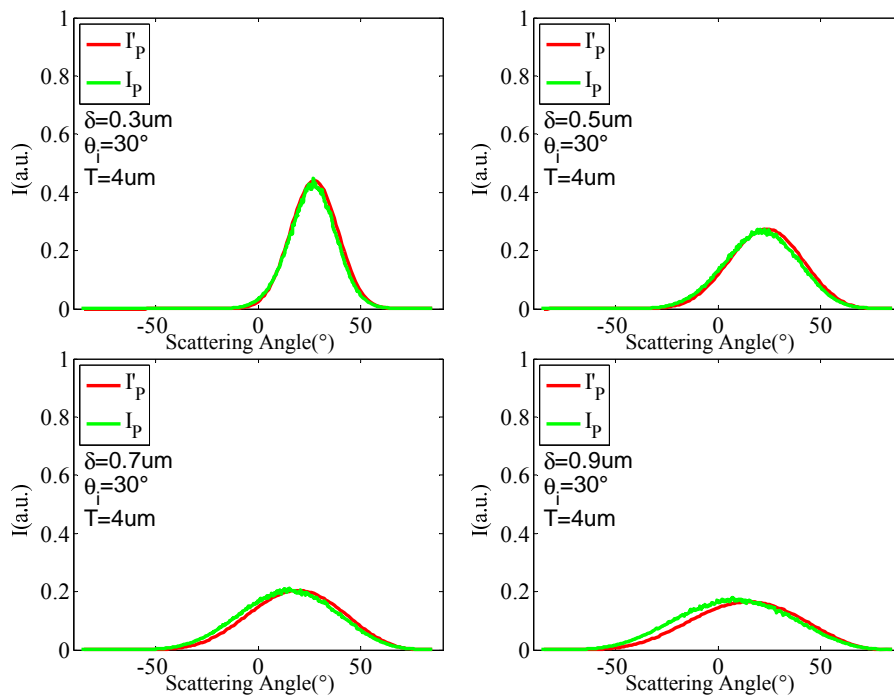


Fig. 9. The comparison between numerical simulation results and theoretical analysis of scattered light intensity from K5 glass dielectric surfaces. Incident light is P light, and the incident angle is 30° , the correlation length $T=4\text{um}$.

4.2. Metal Surfaces

Fig. 10 compares the numerical simulated and theoretical analysis of scattered field of 1-D randomly rough iron metal surfaces when incident light is S light.

Fig. 11 compares the numerical simulated and theoretical analysis of scattered field of 1-D

randomly rough iron metal surfaces when incident light is S light.

According to the comparison between numerical simulation and theoretical analysis shown in Fig. 8 – Fig. 11, it is obvious that the trends of numerical simulation results and theoretical analysis are similar in both randomly rough dielectric and metal surfaces. This illuminate the above analysis is reasonable.

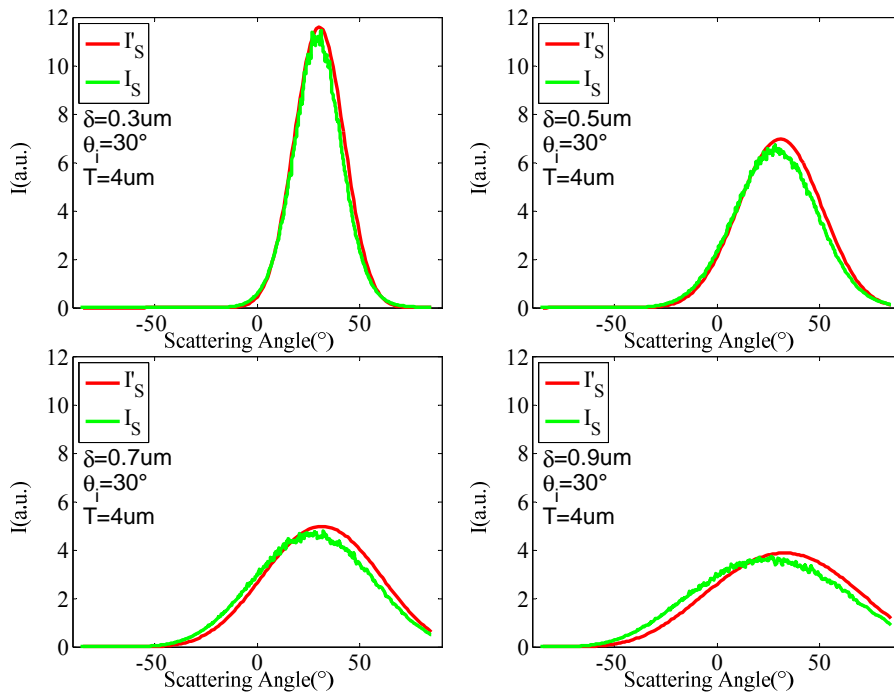


Fig. 10. The comparison between numerical simulation results and theoretical analysis of scattered light intensity from iron metal surfaces. Incident light is S light, and the incident angle is 30° , the correlation length $T=4$ μm .

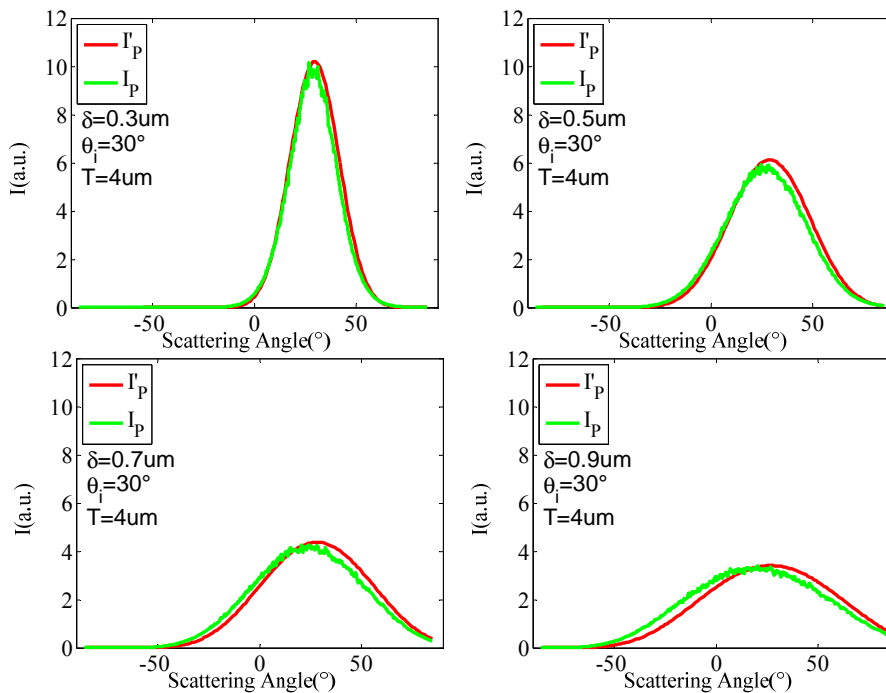


Fig. 11. The comparison between numerical simulation results and theoretical analysis of scattered light intensity from iron metal surfaces. Incident light is S light, and the incident angle is 30° , the correlation length $T=4$ μm .

5. Conclusions

In this paper, scattered light from randomly rough dielectric and metal surfaces are solved by KA. Based on the simulation, we have analyzed the light distribution characteristic by scattered light distribution width, scattered light peak value, and the

peak position. Besides, the simulation clearly shows there is some difference between metal and dielectric surfaces: first, the scattering peak value of metal is larger than scattering peak value of dielectric on the same roughness; secondly, the difference between s- and p-light scattering results are rather small in metal randomly rough surfaces, while there is a

obvious difference between s- and p-polarized scattering results in the condition of dielectric randomly rough surfaces; Thirdly, though in both conditions of metal and dielectric randomly rough surfaces, there is a shift from specular to backscattering direction when incident is p-polarized light, however, in dielectric randomly rough surface situation, the shift is much more obvious than in metal situation.

Moreover, theoretical analysis of the light scattering from randomly rough dielectrics and metal surfaces is proposed in this paper, which explains the changing trends of scattered light intensity at different conditions. Two factors are taken into consideration, and they are local reflectivity and distribution of local slope respectively. The comparison results show that numerical simulated results match well with the theoretical analysis, which shows the accuracy and robustness of the simulation method used in the paper. Both simulation and theoretical analysis could be used as a reference in remote sensing and laser radar, etc.

References

- [1]. A. Ishimaru, Wave propagation and scattering in random media. Volume I - Single scattering and transport theory. Research supported by the US Air Force, NSF, and NIH, *Academic Press, Inc.*, New York, 1978, 267 p.
- [2]. M. A. Lefsky, et al, Lidar remote sensing for ecosystem studies, *BioScience*, Vol. 52, Issue 1, 2002, pp. 19-30.
- [3]. C.-Y. Wang, et al, Optimum signal threshold ratio for improving the ranging accuracy of lidar, *Laser Technology*, Issue 4, 2007, pp. 408-411.
- [4]. J. Deuzé, et al, Remote sensing of aerosols over land surfaces from POLDER-ADEOS-1 polarized measurements, *Journal of Geophysical Research: Atmospheres (1984–2012)*, Vol. 106, Issue D5, 2001, pp. 4913-4926.
- [5]. D. Holliday, Resolution of a controversy surrounding the Kirchhoff approach and the small perturbation method in rough surface scattering theory, *IEEE Transactions on Antennas and Propagation*, Vol. 35, Issue 1, 1987, pp. 120-122.
- [6]. J. Q. Lu, et al., Scattering of light from a rough dielectric film on a reflecting substrate: diffuse fringes, *Journal of the Optical Society of America A*, Vol. 15, Issue 1, 1998, pp. 185-195.
- [7]. P. Tran, V. Celli and A. A. Maradudin, Electromagnetic scattering from a two-dimensional, randomly rough, perfectly conducting surface: iterative methods, *Journal of the Optical Society of America A*, Vol. 11, Issue 5, 1994, pp. 1686-1689.
- [8]. K. Pak, L. Tsang, and J. Johnson, Numerical simulations and backscattering enhancement of electromagnetic waves from two-dimensional dielectric random rough surfaces with the sparse-matrix canonical grid method. *Journal of the Optical Society of America A*, Vol. 14, Issue 7, 1997, pp. 1515-1529.
- [9]. I. Simonsen, A. A. Maradudin, and T. A. Leskova, Scattering of electromagnetic waves from two-dimensional randomly rough perfectly conducting surfaces: The full angular intensity distribution, *Physical Review A*, Vol. 81, Issue 1, 2010, pp. 013806.
- [10]. N. Bruce, and J. Dainty, Multiple scattering from rough dielectric and metal surfaces using the Kirchhoff approximation, *Journal of Modern Optics*, Vol. 38, Issue 8, 1991, pp. 1471-1481.
- [11]. J. E. Harvey, A. Krywonos, and C. L. Vernold, Modified Beckmann-Kirchhoff scattering model for rough surfaces with large incident and scattering angles, *Optical Engineering*, Vol. 46, Issue 7, 2007, pp. 078002-078002.
- [12]. J. A. Stratton, *Electromagnetic theory*, *John Wiley & Sons*, Vol. 33, 2007.
- [13]. J. Shu, et al, Research on generated mechanism of scattering characteristic of random rough dielectric surface, in *Proceedings of the International Society for Optics and Photonics*, Photonics Asia, 2010.
- [14]. S. Jiang, et al, Monte Carlo simulation of Stokes vectors of polarized light scattering from two-dimensional random rough surfaces, *Journal of Modern Optics*, Vol. 58, Issue 18, 2011, pp. 1651-1658.
- [15]. N. Patir, A numerical procedure for random generation of rough surfaces, *Wear*, Vol. 47, Issue 2, 1978, pp. 263-277.
- [16]. J.-J. Wu, Simulation of rough surfaces with FFT, *Tribology International*, Vol. 33, Issue 1, 2000, pp. 47-58.
- [17]. M. J. Weber, *Handbook of optical materials*, *CRC Press*, 2010.